Inorganic Chemistry

Article

pubs.acs.org/IC

A Three-Dimensional Dynamic Metal–Organic Framework with Fourfold Interpenetrating Diamondoid Networks and Selective Adsorption Properties

Ping Ju, Long Jiang, and Tong-Bu Lu*

MOE Key Laboratory of Bioinorganic and Synthetic Chemistry, School of Chemistry and Chemical Engineering, Sun Yat-Sen University, Guangzhou 510275, China

Supporting Information

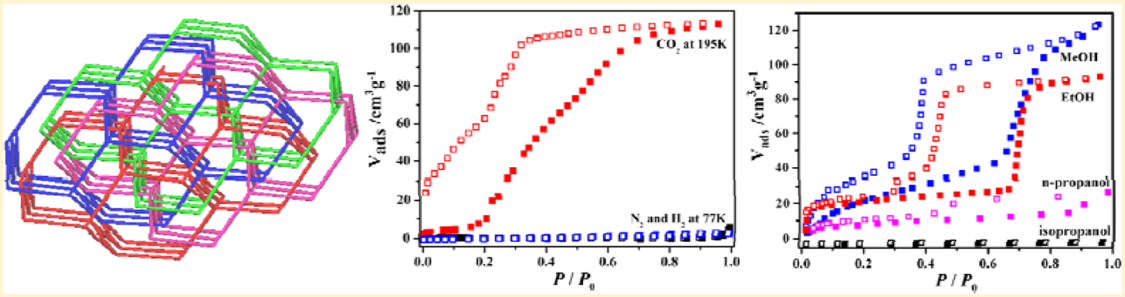

ABSTRACT: A three-dimensional metal–organic framework (**1**) with fourfold interpenetrating diamondoid networks was constructed using a macrocyclic nickel(II) complex and a tetracarboxylic ligand 4,4′,4″,4‴-(cyclohexane-1,2-diyibis(azanetriyl))-tetrakis(methylene)tetrabenzoic acid as building blocks. Despite the fourfold interpenetration, **1** possesses one-dimensional channels that are occupied by water and CH_3CN guest molecules. Once the guest molecules were removed, the framework and pores in desolvated **1** are dynamic with large adsorption hysteresis loops, which exhibit selective gas adsorption for CO_2 at 195 K over N_2 and H_2 at 77 K and selective adsorption for methanol, ethanol, and *n*-propanol over isopropanol at 298 K.

INTRODUCTION

Porous metal–organic frameworks (PMOFs) with well-defined channels have attracted much attention due to their potential applications in gas storage,[1] molecular adsorption and separation,[2] ion exchange,[3] and heterogeneous catalysis.[4] Among these frameworks, dynamic PMOFs, which can transform their structures in response to external stimuli and exploit their porous feature,[5] are considered as a promising class of PMOFs for the development of sensors and gas storage.[6] One of the most interesting phenomena in these dynamic PMOFs is stepwise and selective guest adsorption caused by the guest-induced framework transition, in which the gate of the pores in dynamic PMOFs can be opened by a particular guest molecule, and the design and synthesis of dynamic PMOFs with stepwise and selective guest adsorption behaviors have attracted considerable attention.[7]

Herein, we report the synthesis and structure of an interesting dynamic PMOFs of $[(NiL)_4(CDTA)_2]\cdot 2.5CH_3CN\cdot 22H_2O$ (**1**) with fourfold interpenetrating diamondoid networks, which was constructed using a macrocyclic nickel(II) complex $[NiL]^{2+}$ and a H_4CDTA $[NiL]^{2+}$ semirigid carboxylic ligand H_4CDTA as building blocks (L = 2,2′-(1,3,5,8,10,12-hexaazacyclotetradecane-3,10-diyl)diethanol, H_4CDTA = 4,4′,4″,4‴-(cyclohexane-1,2-diylbis(azanetriyl))tetrakis(methylene)tetrabenzoic acid; see Scheme 1). Interestingly, the desolvated **1** exhibits selective gas sorption properties for CO_2 at 195 K over N_2 and H_2 at 77 K and selective adsorption for methanol, ethanol, and *n*-propanol over isopropanol at 298 K.

Scheme 1. Structures of H_4CDTA and $[NiL]^{2+}$

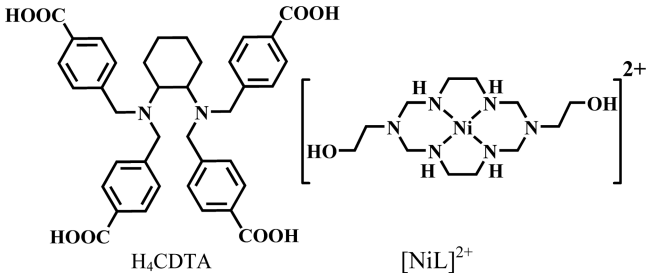

EXPERIMENTAL SECTION

General Methods and Materials. $[NiL](ClO_4)_2$ was prepared according to the literature method.[8] All of the other chemicals are commercially available and used as received. Elemental analyses were determined by an Elemental Vario EL elemental analyzer. Thermogravimetric (TG) curve was recorded on a Netzsch TG 209 instrument under nitrogen atmosphere (heating rate 10 °C/min). The IR spectra in the 4000–400 cm^{-1} region were measured using a

Received: March 15, 2015
Published: June 17, 2015

ACS Publications © 2015 American Chemical Society

DOI: 10.1021/acs.inorgchem.5b00592
Inorg. Chem. 2015, 54, 6291–6295

Bruker EQUINOX 55 spectrometer and KBr pellets. Variable-temperature powder X-ray diffraction measurements were obtained on a Bruker D8 ADVANCE X-ray diffractometer with Cu Kα radiation. ***Caution!*** *Perchlorate salts of metal complexes with organic ligands are potentially explosive. They should be handled with care, and prepared only in small quantities.*

Synthesis of H_4CDTA. The H_4CDTA ligand was prepared according to the following procedure. To a solution of (*R*,*R*)-cyclohexane-1,2-diamine (1.42 g, 10 mmol) and 4-cyanobenzyl bromide (8.82 g, 45 mmol) in 400 mL of CH_3CN was added potassium carbonate (8.29 g, 60 mmol). The suspension was refluxed for 24 h. The solution was filtered and concentrated under vacuum. The resulting reaction mixture was loaded on the top of a silica gel column and eluted with ethyl acetate and petroleum ether to afford the crude product (3.2 g), yield 49%. The obtained solid was dissolved in a mixture solvents of H_2O and ethanol (v/v = 1/1, 200 mL), and a solution of potassium hydroxide (2.5 g, 45 mmol) in water (20 mL) was added. The solution was refluxed overnight and neutralized with HCl (1 M). The resulting precipitate was washed thoroughly with deionized water. The solid was collected and dried to give the product of H_4CDTA (2.2 g, 61%). Electrospray ionization mass spectrometry (ESI-MS) for $C_{38}H_{38}N_2O_8$ (Calcd 650.3): m/z = 651.3 ($[M+1]^+$, 100%); Elemental analysis: calcd for $C_{38}H_{44}N_2O_{11}$ (H_4CDTA·3H_2O): C 64.76, H 6.29, N 3.97%; found: C 65.13, H 6.17, N 4.35%. IR (KBr): ν = 3491 (s), 3066 (m), 2943 (m), 2871 (w), 2643 (w), 2526 (w), 1943 (w), 1702 (vs), 1611 (m), 1556 (w), 1456 (m), 1419 (m), 1377(m), 1284 (vs), 1179 (m), 1120 (m), 1090 (m),1059 (m), 1016 (m), 976 (m), 870 (m), 784 (s), 757 (s), 703 (m), 641 (w), 513 (w) cm^{-1}.

$[(NiL)_4(CDTA)_2]$·2.5CH_3CN·22H_2O (1). An aqueous solution (2 mL) of H_4CDTA (0.02 g, 0.03 mmol) and triethylamine (0.012 g, 0.12 mmol) was layered with an acetonitrile solution (3 mL) of $[NiL](ClO_4)_2$ (0.033 g, 0.06 mmol). Six days later, needle-shaped pink crystals suitable for X-ray analysis formed (8 mg, 15% yield based on $[NiL](ClO_4)_2$). Elemental analysis: calcd for $C_{129}H_{239.5}N_{30.5}Ni_4O_{46}$ (**1**): C 48.59, H 7.57, N 13.40%; found: C 48.94, H 7.11, N 12.95%. IR (KBr): ν = 3361 (vs), 3262 (vs), 2928 (vs), 2867 (vs), 1594 (vs), 1551 (vs), 1456 (m), 1382 (vs), 1292 (w), 1273 (w), 1172 (w), 1056 (m), 1022 (m), 994 (m), 868 (w), 850 (w), 812 (w), 776 (m), 710 (w), 619 (w) cm^{-1}.

Single-Crystal X-ray Crystallography. Single-crystal X-ray diffraction data for **1** were collected on an Agilent Technologies Gemini A Ultra CCD diffractometer with graphite monochromated Cu Kα radiation (λ = 1.541 78 Å) at 150 K. All empirical absorption corrections were applied using the SCALE3 ABSPACK program.[9] The structure was solved by direct method and refined by full-matrix least-squares analysis on F^2 using the SHELX97 program package. All non-hydrogen atoms were refined anisotropically. The guest molecules in **1** could not be successfully located from the different-Fourier map calculation due to the weak diffraction data, and they were treated as a diffuse contribution using the program SQUEEZE;[10] the contents of guest molecules in **1** were deduced by means of EA and TGA. All calculations were performed using the SHELXTL system of computer programs.[11] The crystallographic data for **1** are given in Table 1, and the selected bond lengths and angles are given in Table 2.

Gas Sorption Measurements. The gas sorption experiments were measured using a BELSORP-Max gas adsorption instrument. The N_2, H_2, and CO_2 adsorption isotherms were collected in the 1 × 10^{-4} to 1 atm pressure range. The cryogenic temperature of 77 K required for N_2 and H_2 sorption measurements was controlled using liquid nitrogen bath. The cryogenic temperature of 195 K required for CO_2 sorption measurements was controlled by a dry ice−acetone bath. The temperature for CO_2 sorption measurements (273 K) was controlled by ice bath. The temperature for alcohols sorption measurements (298 K) was controlled using a water bath. The initial sample analysis was performed at 80 °C under a high vacuum (less than 1 × 10^{-6} mbar) for 6 h to remove guest molecules.

Table 1. Crystal Data and Structure Refinement for 1

formula	$C_{129}H_{239.5}N_{30.5}Ni_4O_{46}$	crystal system	orthorhombic
Fw	3188.7	space group	$P2_12_12$
a (Å)	29.042(3)	b (Å)	30.750(5)
c (Å)	9.4483(17)	$\alpha/\beta/\gamma$ (deg)	90/90/90
V (Å^3)	8438(2)	Z	4
D_c (g·cm^{-3})	1.059	reflections/ unique	17 336/11 134
R(int)	0.1392	GOF on F^2	1.096
$R_1[I \geq 2\sigma(I)]$	0.0952	$wR_2[I \geq 2\sigma(I)]$	0.2463
Flack parameter	0.01(2)		

Table 2. Selected Bond Lengths (Å) and Angles (deg) for 1[a]

Ni(1)−N(2)	2.093(14)	Ni(2)−N(8)	2.049(17)
Ni(1)−N(3)	1.960(15)	Ni(2)−N(9)	1.889(17)
Ni(1)−N(5)	2.013(13)	Ni(2)−N(11)	2.104(15)
Ni(1)−N(6)	1.910(15)	Ni(2)- N(12)	2.019(19)
Ni(1)−O(5)	2.131(13)	Ni(2)−O(12)	2.137(14)
Ni(1)−O(7)#2	2.215(13)	Ni(2)−O(9)#3	2.113(14)
Ni(1)#4-O(7)	2.215(13)	Ni(2)#1−O(9)	2.113(14)
N(3)−Ni(1)−N(2)	86.0(4)	N(8)−Ni(2)−N(11)	179.3(6)
N(3)−Ni(1)−N(5)	91.9(4)	N(9)−Ni(2)−N(8)	88.1(6)
N(5)−Ni(1)−N(2)	177.7(5)	N(9)−Ni(2)−N(11)	91.4(5)
N(6)−Ni(1)−N(2)	94.1(5)	N(9)−Ni(2)−N(12)	177.4(6)
N(6)−Ni(1)−N(3)	179.(7)	N(12)−Ni(2)−N(8)	94.0(5)
N(6)−Ni(1)−N(5)	88.1(5)	N(12)−Ni(2)−N(11)	86.5(5)
N(2)−Ni(1)−O(5)	92.2(5)	N(8)−Ni(2)−O(9)#3	92.6(6)
N(2)−Ni(1)−O(7)#2	85.5(5)	N(8)−Ni(2)−O(12)	90.3(6)
N(3)−Ni(1)−O(5)	93.2(5)	N(9)−Ni(2)−O(9)#3	91.4(7)
N(3)−Ni(1)−O(7)#2	85.7(5)	N(9)−Ni(2)−O(12)	90.7(7)
N(5)−Ni(1)−O(5)	88.6(5)	N(11)−Ni(2)−O(9)#3	87.9(6)
N(5)−Ni(1)−O(7)#2	93.7(5)	N(11)−Ni(2)−O(12)	89.2(5)
N(6)−Ni(1)−O(5)	86.2(6)	N(12)−Ni(2)−O(9)#3	87.0(6)
N(6)−Ni(1)−O(7)#2	94.9(6)	N(12)−Ni(2)−O(12)	90.9(6)
O(5)−Ni(1)−O(7)#2	177.5(5)	O(9)#3-Ni(2)−O(12)	176.6(6)

[a]Symmetry codes: #1 $x - 1/2, -y + 1/2, -z$; #2 $-x + 3/2, y - 1/2, -z + 2$; #3 $x + 1/2, -y + 1/2, -z$.

RESULTS AND DISCUSSION

Description of the Structure. The result of X-ray structural analysis reveals that **1** crystallizes in orthorhombic crystal system, with a chiral space group of $P2_12_12$. The asymmetric unit of **1** contains two independent Ni(II) ions, and each Ni(II) is six-coordinated to four nitrogen atoms from L and two carboxylate oxygen atoms from two individual $CDTA^{4-}$ anions, forming a slightly distorted N_4O_2 octahedral geometry (Figure 1a). The Ni−N distances in the equatorial plane are between 1.889(17) and 2.104(15) Å; the Ni−O distances in axial positions are between 2.113(14) and 2.215(13) Å. As shown in Figure 1b, 12 $[NiL]^{2+}$ are bridged by 10 $CDTA^{4-}$ to construct a diamondoid cage. The diamondoid cages are further connected through the coordination interactions between $CDTA^{4-}$ and $[NiL]^{2+}$ to form a three-dimensional (3D) diamondoid network (Figure 1b,c). The diamondoid cage exhibits maximum dimensions of 27 × 42 × 40 Å^3 (the longest intracage distances, Figure 1b).[12] Such a large cavity of the diamondoid cage causes the fourfold interpenetration of the networks (Figure 1d), generating two kinds of one-dimensional (1D) channels along the *c*-axis, the rectangular and rhombohedral channels, with the sizes of 6 × 8 Å^2 and 3 × 30 Å^2, respectively (Figure 1e). Solvent molecules

DOI: 10.1021/acs.inorgchem.5b00592
Inorg. Chem. 2015, 54, 6291−6295

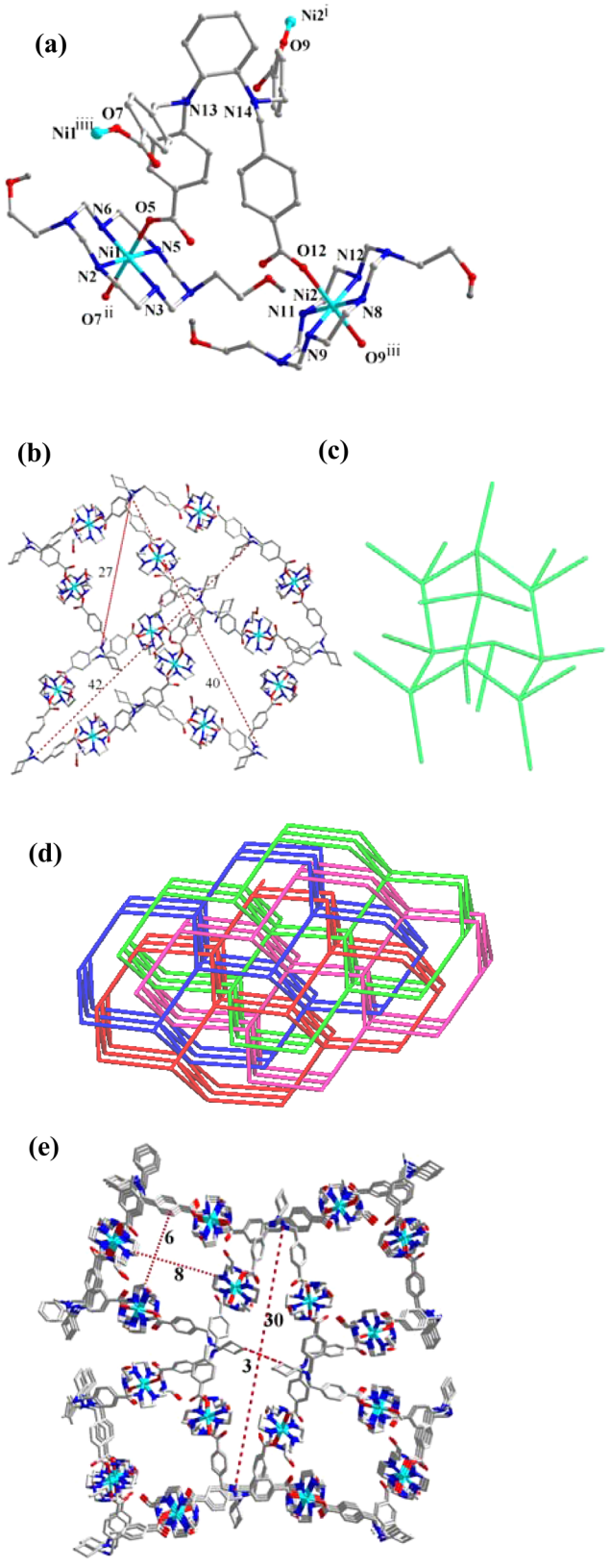

Figure 1. (a) Coordination environments of Ni(II) and $CDTA^{4-}$ in **1** (symmetry codes: (i) $x - 1/2, -y + 1/2, -z$; (ii) $-x + 3/2, y - 1/2, -z + 2$; (iii) $x + 1/2, -y + 1/2, -z$; (iiii) $-x + 3/2, y + 1/2, -z + 2$). (b) The view of a diamondoid cage and (c) a schematic illustration of the diamondoid cage. (d) Fourfold interpenetrating diamondoid networks. (e) 3D structure with 1D channels in **1**.

are filled in the channels, and ~29% solvent-accessible volume was estimated by using the PLATON program.[13]

Thermal Analysis and Powder X-ray Diffraction. To evaluate the stability of **1**, thermogravimetric analysis (TGA) was performed. A weight loss of 15.1% was observed from room temperature to 75 °C in the TG curve (Supporting Information, Figure S1), corresponding to the release of MeCN and water guest molecules (calcd 15.6%) in the channels. The desolvated **1** is stable up to 200 °C, followed by additional weight losses after that temperature. Variable-temperature PXRD for **1** was measured from room temperature to 230 °C under nitrogen atmosphere (Figure 2a). The results show

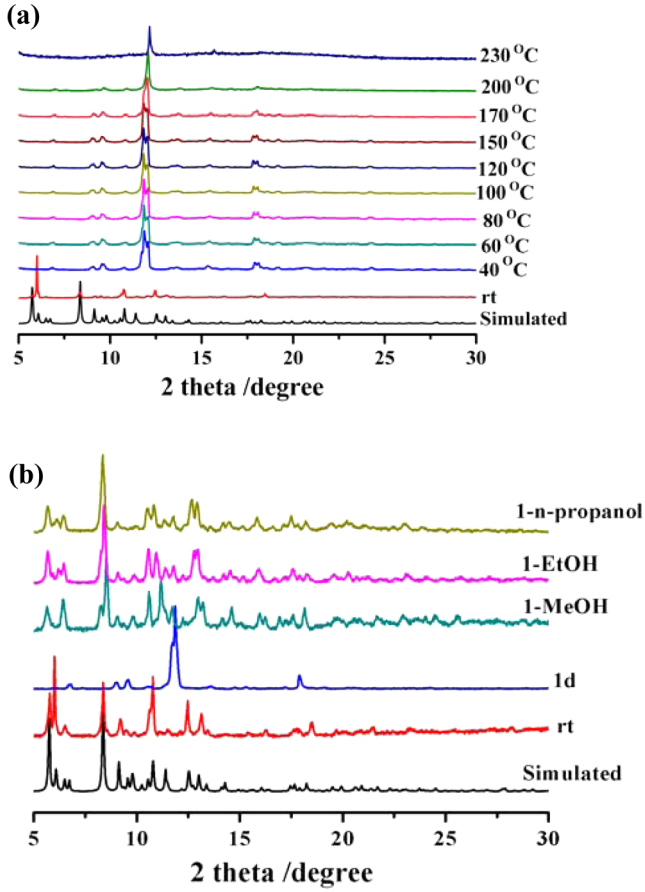

Figure 2. (a) Variable-temperature XRD patterns for **1**. (b) XRD patterns for simulated from X-ray crystal diffraction data, as synthesized, **1d**, and immersing **1d** in methanol, ethanol, and *n*-propanol, respectively.

that the XRD pattern of **1** was changed when the sample was heated to 40 °C (Figure 2a). This can be attributed to the shrinkage of the fourfold interpenetrating diamondoid networks after the remove of guest molecules. When **1d** was immersed in methanol, ethanol, and *n*-propanol at 30 °C for 2 min, the original structure of **1** was recovered as evidenced by PXRD patterns (Figure 2b). The framework of **1d** can be stable up to 200 °C, which is consistent with the result of TGA.

Gas Adsorption. To evaluate the permanent porosity of **1**, gas adsorption studies were performed on the desolvated sample (**1d**). It is interesting to note that **1d** can hardly adsorb N_2 and H_2 at 77 K, while it can adsorb CO_2 at 195 K in the 1×10^{-4} to 1 atm pressure range (Figure 3a), indicating the gate of the pores in **1d** can only be opened by CO_2; thus, **1d** can

DOI: 10.1021/acs.inorgchem.5b00592
Inorg. Chem. 2015, 54, 6291−6295

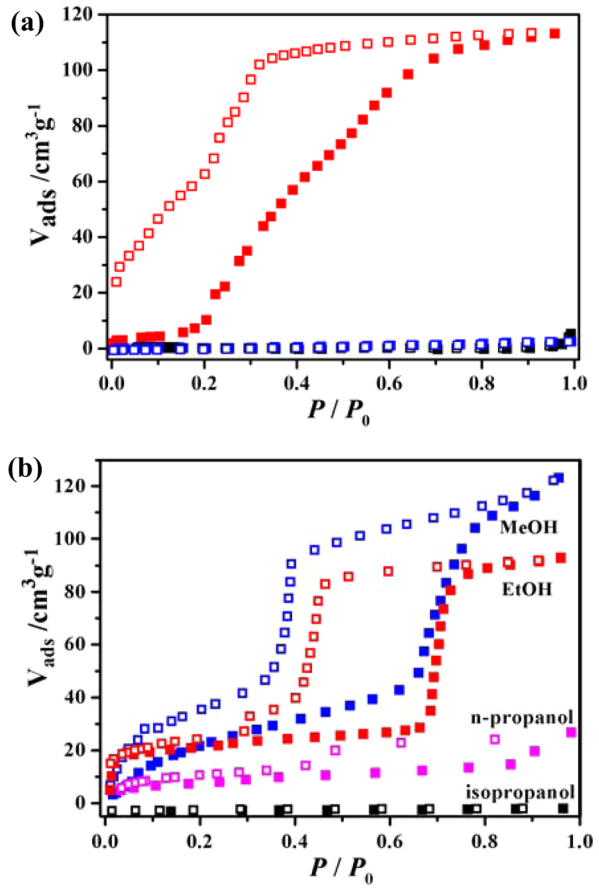

Figure 3. (a) Gas adsorption isotherms of **1d** for CO_2 (red) at 195 K and N_2 (blue) and H_2 (black) at 77 K. (b) Gas adsorption isotherms of **1d** for MeOH (blue), EtOH (red), *n*-propanol (magenta), and isopropanol (black) measured at 298 K. Filled shapes: adsorption, open shapes: desorption.

selectively adsorb CO_2 over N_2 and H_2. The above adsorption behavior can be ascribed to the quadrupole moment of CO_2 (-1.4×10^{-39} cm^2),[14] which induces interaction with the framework to open the channels,[15] while the pores in **1d** can not be opened by N_2 and H_2 even at 77 K due to the lack of such interactions. The sorption isotherm of CO_2 shows a two-step sorption at 195 K, **1d** can only adsorb 5.84 cm^3 (STP)/g of CO_2 from 0 to 0.15 atm (the gate-opening pressure), and then it starts to adsorb CO_2 and gradually reaches 113 cm^3 (STP)/g (22.1 wt %) at 0.95 atm. It is interesting to see that the desorption isotherm does not coincide with the adsorption isotherm (Figure 3a), and **1d** shows almost no desorption until the pressure was less than 0.35 atm, and then abruptly desorbed, resulting in a significantly large adsorption hysteresis. The absorbed CO_2 can not be completely released even at near zero atmospheres (Figure 3a), indicating a strong interaction between CO_2 and framework in **1d** at 195 K. The above stepwise adsorption behavior and large adsorption hysteresis demonstrate the pores in **1d** is dynamic. At lower pressure, the gate of pores in **1d** is almost closed after the removal of guest molecules; thus, **1d** shows a quite small adsorption, while the adsorbed limited CO_2 molecules can open the gate of the pores through the "host−guest" interactions between CO_2 and the hydroxyl and secondary amino groups located on the surface of the pores in **1d** to allow more CO_2 molecules to enter.[16] It is interesting to note that CO_2 molecules cannot open the gate of the pores at 273 K, the sorption isotherm of CO_2 does not show an obvious adsorption hysteresis loop at 273 K (Supporting Information, Figure S2), and **1d** can only adsorb 10.054 cm^3 (STP)/g of CO_2 at 0.95 atm; this value is much smaller than the corresponding value of 113 cm^3 (STP)/g adsorbed at 195 K, indicating the pores in **1d** cannot be opened by CO_2 at 273 K, as the interactions between CO_2 and the framework of **1d** become weaker at higher temperature (273 K). Although the CO_2 adsorption capability of **1d** is not as high as some reported MOFs, such as $Zn_2(BPnDC)_2(bpy)$ (SNU-9, 190 cm^3 (STP)/g at 195 K and 1.0 atm) and NOTT-202a (321 cm^3 (STP)/g, at 195 K and 1.0 atm),[17] the high selective gas sorption behavior of **1d** for CO_2 over N_2 suggests that **1d** can be used for CO_2 capture and separation.[18]

To further study the sorption properties of dynamic pores in **1d**, a series of alcohol sorption measurements were obtained in the 0.01 to 1 atm pressure range. The results indicated that **1d** can selectively adsorb methanol, ethanol, and *n*-propanol over isopropanol (Figure 3b). Interestingly, the adsorption isotherms of methanol and ethanol at 298 K also show obvious stepwise adsorption behavior, and the desorption isotherms exhibit large hysteresis loops. The large hysteresis and stepwise process of methanol and ethanol adsorption profiles of **1d** are characteristic of the dynamic PMOFs. Approximately 7.4 MeOH, 5.6 EtOH, and 1.6 *n*-propanol molecules are adsorbed per formula unit at 1 atm. The numbers of absorbed alcohols decreased along with increasing sizes from methanol to *n*-propanol, indicating the absorption of alcohols is size-dependent.[19] The absence of isopropanol adsorption by **1d** demonstrates that isopropanol is too large to enter the dynamic channels of **1d**, and **1d** can be used for the separation of *n*-propanol and isopropanol.

CONCLUSIONS

In conclusion, a unique 3D PMOF with fourfold interpenetrating diamondoid networks and 1D channels based on a tetracarboxylate ligand and an azamacrocyclic Ni(II) complex has been successfully synthesized and structurally characterized. The desolvated **1** exhibits selective gas adsorption for CO_2 over N_2 and H_2 and selective adsorption for methanol, ethanol, and *n*-propanol over isopropanol. The large hysteresis loops for CO_2 and alcohols adsorption were observed, demonstrating the framework and pores of **1d** are dynamic. The above selective adsorption behaviors can be used for CO_2 capture and separation, as well as for the separation of the isomers of propanol.

ASSOCIATED CONTENT

Supporting Information

TGA curve for **1** and gas adsorption isotherm of **1d** for CO_2 at 273 K. The Supporting Information is available free of charge on the ACS Publications website at DOI: 10.1021/acs.inorgchem.5b00592.

AUTHOR INFORMATION

Corresponding Author

*E-mail: lutongbu@mail.sysu.edu.cn. Fax: +86-20-84112921.

Notes

The authors declare no competing financial interest.

DOI: 10.1021/acs.inorgchem.5b00592
Inorg. Chem. 2015, 54, 6291−6295

■ ACKNOWLEDGMENTS

This work was supported by 973 Program of China (2012CB821706, 2014CB845602), NSFC (Grant No. 21331007), and NSF of Guangdong Province (S2012030006240).

■ REFERENCES

(1) (a) Chen, Y. Q.; Qu, Y. K.; Li, G. R.; Zhuang, Z. Z.; Chang, Z.; Hu, T. L.; Xu, J.; Bu, X. H. *Inorg. Chem.* **2014**, *53*, 8842−8844. (b) Niu, Z.; Fang, S.; Ma, J. G.; Zhang, X. P.; Cheng, P. *Chem. Commun.* **2014**, *50*, 7797−7799. (c) Rosi, N. L.; Eckert, J.; Eddaoudi, M.; Vodak, D. T.; Kim, J.; O'keeffe, M.; Yaghi, O. M. *Science* **2003**, *300*, 1127−1129. (d) Chen, B.; Ockwig, N. W.; Millward, A. R.; Contreras, D. S.; Yaghi, O. M. *Angew. Chem.* **2005**, *117*, 4823−4827. (e) Wong-Foy, A. G.; Matzger, A.; Yaghi, O. M. *J. Am. Chem. Soc.* **2006**, *128*, 3494−3495.

(2) (a) Hou, C.; Liu, Q.; Okamura, T.; Wang, P.; Sun, W. Y. *CrystEngComm* **2012**, *14*, 8569−8576. (b) Alawisi, H.; Li, B.; He, Y. B.; Arman, H. D.; Asiri, A. M.; Wang, H. L.; Chen, B. L. *Cryst. Growth Des.* **2014**, *14*, 2522−2526. (c) Xuan, W. M.; Zhang, M. N.; Liu, Y.; Chen, Z. J.; Cui, Y. *J. Am. Chem. Soc.* **2012**, *134*, 6904−6907. (d) Choi, H. J.; Suh, M. P. *J. Am. Chem. Soc.* **2004**, *126*, 15844−15851. (e) Zhang, Z. J.; Yao, Z. Z.; Xiang, S. C.; Chen, B. L. *Energy Environ. Sci.* **2014**, *7*, 2868−2899.

(3) (a) Zhang, Z. J.; Shi, W.; Niu, Z.; Li, H. H.; Zhao, B.; Cheng, P.; Liao, D. Z.; Yan, S. P. *Chem. Commun.* **2011**, *47*, 6425−6427. (b) Gao, L.; Li, C. Y. V.; Chan, K. Y.; Chen, Z. N. *J. Am. Chem. Soc.* **2014**, *136*, 7209−7212.

(4) (a) Wu, C. D.; Hu, A.; Zhang, L.; Lin, W. B. *J. Am. Chem. Soc.* **2005**, *127*, 8940−8941. (b) Liu, Y.; Xi, X. B.; Ye, C. C.; Gong, T. F.; Yang, Z. W.; Cui, Y. *Angew. Chem., Int. Ed.* **2014**, *53*, 14041−14045. (c) Peng, Y. W.; Gong, T. F.; Cui, Y. *Chem. Commun.* **2013**, *49*, 8253−8255. (d) Gomez-Lor, B.; Gutierrez-Puebla, E.; Iglesias, M.; Monge, M. A.; Ruiz-Valero, C.; Snejko, N. *Chem. Mater.* **2005**, *17*, 2568−2573. (e) He, H. Y.; Ma, H. Q.; Sun, D.; Zhang, L. L.; Wang, R. M.; Sun, D. F. *Cryst. Growth Des.* **2013**, *13*, 3154−3161.

(5) (a) Kitagawa, S.; Uemura, K. *Chem. Soc. Rev.* **2005**, *34*, 109−119. (b) Fletcher, A. J.; Thomas, K.; Rosseinsky, M. *J. Solid State Chem.* **2005**, *178*, 2491−2510. (c) Devic, T.; Horcajada, P.; Serre, C.; Salles, F.; Maurin, G.; Moulin, B.; Heurtaux, D.; Clet, G.; Vimont, A.; Grenèche, J. M.; Ouay, B. L.; Moreau, F.; Magnier, E.; Filinchuk, Y.; Marrot, J.; Lavalley, J. C.; Daturi, M.; Fèrey, G. *J. Am. Chem. Soc.* **2010**, *132*, 1127−1136. (d) Llewellyn, P. L.; Bourrelly, S.; Serre, C.; Filinchuk, Y.; Fèrey, G. *Angew. Chem.* **2006**, *118*, 7915−7918. (e) Serre, C.; Mellot-Draznieks, C.; Surblé, S.; Audebrand, N.; Filinchuk, Y.; Férey, G. *Science* **2007**, *315*, 1828−1831. (f) He, Y. P.; Tan, Y. X.; Zhang, J. *J. Mater. Chem. C* **2014**, *2*, 4436−4441.

(6) (a) Gong, Y. N.; Jiang, L.; Lu, T. B. *Chem. Commun.* **2013**, *49*, 11113−11115. (b) Lv, G. C.; Wang, P.; Liu, Q.; Fan, J.; Chen, K.; Sun, W. Y. *Chem. Commun.* **2012**, *48*, 10249−10251. (c) Li, Y. W.; Li, J. R.; Wang, L. F.; Zhou, B. Y.; Chen, Q.; Bu, X. H. *J. Mater. Chem. A* **2013**, *1*, 495−499. (d) Su, Z.; Chen, M.; Okamura, T.; Chen, M. S.; Chen, S. S.; Sun, W. Y. *Inorg. Chem.* **2011**, *50*, 985−991. (e) Ma, S. Q.; Sun, D. F.; Yuan, D. Q.; Wang, X. S.; Zhou, H. C. *J. Am. Chem. Soc.* **2009**, *131*, 6445−6451. (f) Cui, P.; Ma, Y. G.; Li, H. H.; Zhao, B.; Li, J. R.; Cheng, P.; Balbuena, P. B.; Zhou, H. C. *J. Am. Chem. Soc.* **2012**, *134*, 18892−18895.

(7) (a) Meng, X. R.; Zhong, D. C.; Jiang, L.; Li, H. Y.; Lu, T. B. *Cryst. Growth Des.* **2011**, *11*, 2020−2025. (b) Jiang, L.; Ju, P.; Meng, X. R.; Kuang, X. J.; Lu, T. B. *Sci. Rep.* **2012**, *2*, 668−772. (c) Ju, P.; Jiang, L.; Lu, T. B. *Chem. Commun.* **2013**, *49*, 1820−1822. (d) Venna, S. R.; Carreon, M. A. *Langmuir* **2011**, *27*, 2888−2894. (e) Kitaura, R.; Seki, K.; Akiyama, G.; Kitagawa, S. *Angew. Chem., Int. Ed.* **2003**, *42*, 428−431. (f) Serre, C.; Bourrelly, S.; Vimont, A.; Ramsahye, N. A.; Maurin, G.; Llewellyn, P. L.; Daturi, M.; Filinchuk, Y.; Leynaud, O.; Barnes, P.; Férey, G. *Adv. Mater.* **2007**, *19*, 2246−2251. (g) Tanaka, D.; Nakagawa, K.; Higuchi, M.; Horike, S.; Kubota, Y.; Kobayashi, T. C.; Takata, M.; Kitagawa, S. *Angew. Chem.* **2008**, *120*, 3978−3982. (h) Kubota, Y.; Takata, M.; Matsuda, R.; Kitaura, R.; Kitagawa, S.; Kobayashi, T. C. *Angew. Chem.* **2006**, *118*, 5054−5058. (i) Chen, M. S.; Chen, M.; Takamizawa, S.; Okamura, T.; Fana, J.; Sun, W. Y. *Chem. Commun.* **2011**, *47*, 3787−3789.

(8) Choi, H. J.; Suh, M. P. *Inorg. Chem.* **1999**, *38*, 6309−6312.

(9) Sheldrick, G. M. *SADABS, Program for Empirical Absorption Correction of Area Detector Data;* University of Göttingen: Göttingen, Germany, 1996.

(10) Sluis, P. van der.; Spek, A. L. *Acta Crystallogr.* **1990**, *A46*, 194−201.

(11) Sheldrick, G. M. *SHELXS 97, Program for Crystal Structure Refinement;* University of Göttingen: Göttingen, Germany, 1997.

(12) (a) Cheon, Y. E.; Suh, M. P. *Chem.—Eur. J.* **2008**, *14*, 3961−3967. (b) Kim, H. J.; Suh, M. P. *Inorg. Chem.* **2005**, *44*, 810−812.

(13) Spek, A. L. *J. Appl. Crystallogr.* **2003**, *36*, 7−13.

(14) (a) Coriani, S.; Halkier, A.; Rizzo, A.; Ruud, K. *Chem. Phys. Lett.* **2000**, *326*, 269−276. (b) Choi, H. S.; Suh, M. P. *Angew. Chem., Int. Ed.* **2009**, *48*, 6865−6869. (c) Du, M.; Li, C. P.; Chen, M.; Ge, Z. W.; Wang, X.; Wang, L.; Liu, C. S. *J. Am. Chem. Soc.* **2014**, *136*, 10906−10909.

(15) Seo, J.; Matsuda, R.; Sakamoto, H.; Bonneau, C.; Kitagawa, S. *J. Am. Chem. Soc.* **2009**, *131*, 12792−12800.

(16) (a) Chen, Z. X.; Xiang, S. C.; Arman, H. D.; Mondal, J. U.; Li, P.; Zhao, D. Y.; Chen, B. L. *Inorg. Chem.* **2011**, *50*, 3442−3446. (b) Lee, C. H.; Tsai, M. R.; Chang, Y. T.; Lai, L. L.; Lu, K. L.; Cheng, K. L. *Chem.—Eur. J.* **2013**, *19*, 10573−10579. (c) Xiang, Z. H.; Leng, S. H.; Cao, D. P. *J. Phys. Chem. C* **2012**, *116*, 10573−10579.

(17) (a) Volodymyr, B.; Irena, S.; Dirk, W.; Daniel, M. T.; Ivo, Z.; Ralf, F.; Uwe, M.; Stefan, K. *Inorg. Chem.* **2014**, *53*, 1513−1520. (b) Yang, S. H.; Lin, X.; Lewis, W.; Suyetin, M.; Bichoutskaia, E.; Parker, J. E.; Tang, C. C.; Allan, D. R.; Rizkallah, P. J.; Hubberstey, P.; Champness, N. R.; Thomas, K. M.; Blake, A. J.; Schröder, M. *Nat. Mater.* **2012**, *11*, 710−716. (c) Ma, S. Q.; Zhou, H. C. *Chem. Commun.* **2010**, *46*, 44−53.

(18) (a) Li, J. R.; Kuppler, R. J.; Zhou, H. C. *Chem. Soc. Rev.* **2009**, *38*, 1477−1504. (b) Horike, S.; Kishida, K.; Watanabe, Y.; Inubushi, Y.; Umeyama, D.; Sugimoto, M.; Fukushima, T.; Inukai, M.; Kitagawa, S. *J. Am. Chem. Soc.* **2012**, *134*, 9852−9855.

(19) Chen, S. S.; Chen, M.; Takamizawa, S.; Wang, P.; Lv, G. C.; Sun, W. Y. *Chem. Commun.* **2011**, *47*, 4902−4904.

DOI: 10.1021/acs.inorgchem.5b00592
Inorg. Chem. 2015, 54, 6291−6295